Experimental Evaluation of 5G Modulation Schemes in Quasi-Static Scenarios

Tomás Domínguez-Bolaño, José Rodríguez-Piñeiro, José A. García-Naya, and Luis Castedo
University of A Coruña, A Coruña, Spain
{tomas.bolano, j.rpineiro, jagarcia, luis}@udc.es

***Abstract*—Orthogonal Frequency-Division Multiplexing (OFDM) is a widely used modulation scheme in wireless communications due to its robustness against channel multi-path. Unfortunately, the time-domain rectangular-shape of the OFDM-modulated symbols yields a frequency response with high side lobes, thus producing co-channel interference. More recently, Filter Bank Multicarrier (FBMC) modulation schemes have been proposed as an alternative to OFDM due to their better spectral efficiency and more degrees of freedom to define well localized prototype filters.**

In this paper, the performance of two common prototype filters for an FBMC scheme, known also as Staggered Multitone (SMT), is analyzed analytically and by means of computer simulations considering standardized channel models. The results are also compared to OFDM. Finally it is experimentally evaluated through over-the-air transmissions in different environments using a custom-developed testbed. Performance results, in terms of the Bit Error Ratio (BER) with respect to the average signal-to-noise ratio, show a similar performance for OFDM and FBMC in all the cases. This is mainly because the considered channel models and measurement scenarios are quasi-static and we have considered an isolated point-to-point link, thus not including potential advantages of FBMC schemes, which can be exploited without additional performance losses with respect to OFDM.

I. Introduction

Orthogonal Frequency-Division Multiplexing (OFDM) is currently one of the most used Multi Carrier Modulation (MCM) schemes for wireless communications. This is due to its several advantages, among which some of the most remarkable ones are its robustness against multi-path propagation (frequency-selective channels), and that it can be implemented very efficiently using an Inverse Fast Fourier Transform (IFFT) block at the transmitter, a Fast Fourier Transform (FFT) block at the receiver, and a single tap per subcarrier Zero-Forcing (ZF) equalizer. However, the robustness against multi-path channels is achieved by inserting a Cyclic Prefix (CP) to each OFDM symbol, which reduces the spectral efficiency, and the time-domain rectangular-shape of the symbols leads to an infinitely long frequency response.

Over the last few years, schemes based on Filter Bank Multicarrier (FBMC) using Offset Quadrature Amplitude Modulation (OQAM) have received some attention as a promising alternative to OFDM [1]. In OQAM a time-offset of half the Quadrature Amplitude Modulation (QAM) symbol duration is introduced between the real and the imaginary parts. These systems are known as FBMC/OQAM or OFDM/OQAM [2]. The more concise name Staggered Multitone (SMT) has also been suggested recently [1].

Compared to OFDM, SMT systems do not use a CP, so they may provide a higher useful bit rate. The considered prototype filter can be adapted to the time and frequency dispersion characteristics of the given channel, thus these systems can offer a more localized frequency response, yielding a better performance in some situations (e.g. doubly dispersive channels). Finally, SMT systems can be also implemented efficiently using an IFFT block at the transmitter and a FFT block at the receiver [3].

However, channel estimation in SMT is more difficult than in OFDM. In OFDM scattered pilots are commonly inserted among the data symbols and, since the OFDM symbols are orthogonal, the pilot symbols can be recovered ideally without interference and the channel can be estimated easily. In SMT, the real and imaginary parts of the QAM symbols are separated and transmitted as a pair of Pulse Amplitude Modulation (PAM) symbols, but unlike OFDM, the orthogonality only holds for the real part [4]. The symbols recovered at the receiver are complex-valued and the imaginary part is due to the channel effect plus interferences from the surrounding symbols. Hence the channel cannot be estimated directly even in the case of an ideal channel. To overcome this problem, several channel estimation methods have been proposed in the literature. In [4], one symbol adjacent to each pilot is employed to cancel the interference of the imaginary part. This adjacent symbol was named later in [5] as Auxiliary Pilot (AP). More recently [6], a more complex method named Coded Auxiliary Pilot (CAP) was proposed. This method is based on the same idea of canceling the interference, but in this case a linear coding is applied to the data symbols surrounding the pilot. As shown in [6], the AP takes up a significant amount of power overhead to cancel the interference, which can be reduced significantly by applying the proposed CAP method.

Several comparisons between the performance of OFDM and FBMC are available in the literature [7]–[10]. However, to the best knowledge of the authors, most of them are solely based on analytic and/or simulation-based results. The main contribution of this paper is the experimental evaluation (by means of over-the-air transmissions) of two of the proposed prototype filters for SMT systems, namely the one defined by the PHYDYAS project [11] and the so-called Hermite pulse [12]. Performance will be evaluated over quasi-static scenarios in terms of Bit Error Ratio (BER) against the E_b/N_0 at the receiver. The performance of OFDM will also be included for comparison purposes. Simulation results based on channel

models standardized by the 3rd Generation Partnership Project (3GPP) are also included.

II. SMT Signal Model

In this section we describe the signal model used in our simulations and experimental evaluations. We consider a SMT scheme using N subcarriers and transmitting P time-domain symbols per subcarrier. We denote $\mathcal{A}$ as the set of subcarriers utilized by the system, with values between 0 and $N-1$.

The discrete-time baseband SMT modulated signal is

$$s[k] = \sum_{p=0}^{P-1} \sum_{l \in \mathcal{A}} a_{l,p} g\left[k - p\frac{N}{2}\right] \exp\left(j\phi_{l,p}\right) \exp\left(jl\frac{2\pi}{N}k\right),$$

where $g[k]$ is the discrete-time prototype filter used, $a_{l,p}$ is the transmitted PAM symbol for time p and subcarrier l, and $\phi_{l,p} = \frac{\pi}{2}(l+p)$.

The signal $s[k]$ is sent by the transmitter, passes through a physical channel and is affected by Additive White Gaussian Noise (AWGN) resulting in the received signal $r[k]$, which is modeled as

$$r[k] = \sum_{\tau} h[k,\tau] * s[k-\tau] + w[k],$$

where $h[k,\tau]$ is the discrete-time channel impulse response, $w[k]$ is the uncorrelated complex-valued AWGN with variance σ_w^2, and $*$ denotes the convolution operation.

For each subcarrier m at the receiver, $r[k]$ is first down-converted multiplying by $\exp\left(-jm\frac{2\pi}{N}k\right)$ and filtered by the matched filter $\hat{g}[k]$ to obtain the signal

$$y_m[k] = r[k] \exp\left(-jm\frac{2\pi}{N}k\right) * \hat{g}[k].$$

Finally, the symbols $a_{l,p}$ are recovered as

$$\hat{a}_{l,p} = \Re\left\{\exp\left(-j\phi_{l,p}\right) y_l\left[p\frac{N}{2}\right]\right\}.$$

For our evaluations, we consider $g[k]$ as the prototype filters defined by the PHYDYAS project [11] and the so-called Hermite pulse [12]. For these filters the receiver matched filter will be the same as the transmitter filter, i.e., $\hat{g}[k] = g[k]$, since they are symmetric in the time domain.

III. Evaluation Setup

We use the evaluation setup shown in Fig. 1. Two main branches can be distinguished, labeled as "measurements branch" and "simulations branch". On the one hand, the "measurements branch" implies using the GTEC Testbed (see Section III-C) to measure through an actual wireless channel. On the other hand, the "simulations branch" only includes a channel model, with the purpose of performing evaluations by simulations.

A. Signal Generation and Signal Processing

In this section, the high-level software part of the setup used for the evaluations is introduced, namely the blocks labeled "signal generation" and "signal processing" in Fig. 1.

At the transmitter side, SMT-modulated signals are generated using a custom-developed SMT signal generator. It is worth noting that the Hermite pulse is specially suitable for multicarrier transmissions over doubly dispersive channels because of its good localization in time and frequency [12]. Our signal generator also supports OFDM signals (which correspond to the use of a rectangular filter in the time domain). At the receiver side, a custom-developed SMT receiver is used. Such a receiver includes:

- **Basic channel estimation**: the channel response is estimated by means of a rectangular grid of pilots. For SMT signals, the receiver has to deal with the interference caused by the lack of orthogonality of the received signal, since only orthogonality in the real part is ensured [1]. Several methods that minimize the effect of the interference based on the so-called auxiliary pilot schemes were implemented [4]–[6]. For the results shown in this paper, the so-called CAP method [6] (using 8 symbols around each pilot) is used.
- **Basic channel interpolation**: a two-dimensional (time and frequency) interpolation technique based on the use of cubic splines is used.
- **Basic channel equalization**: a basic ZF equalizer was implemented. We chose this equalizer because of its simplicity and because with a ZF equalizer the equalization procedure is the same for both OFDM and SMT.

Time and frequency synchronization algorithms are also implemented. However, in order to avoid distorting the results shown in this paper, perfect time and frequency synchronization was considered for the simulations, whereas near-perfect frequency synchronization is considered for the measurements.

B. Channel Model

Channel models were used to perform the evaluations based on simulations. We select noise variance values that lead to the desired E_b/N_0 values. The following channel models are considered: the Typical Urban channel model (TUx) for deployment evaluation specified by the 3GPP [13]; Indoor Office B (IBx) and Outdoor-to-Indoor and Pedestrian A (PAx), both from the ITU Radiocommunication Sector (ITU-R) third generation (3G) channel models [14]. The Doppler spread parameter of the channel models was set according to the carrier frequency as well as the desired speed. We consider static scenarios (0 km/h) as well as pedestrian mobility (3 km/h). While the TUx models situations in which the receiver is in a urban area, the IBx is more suitable for indoor transmissions. Finally, the PAx considers an outdoor-to-indoor scenario. These scenarios are the most typical ones for a pedestrian user.

The Power Delay Profile (PDP) and the frequency response of the considered channel models is shown in Fig. 2.

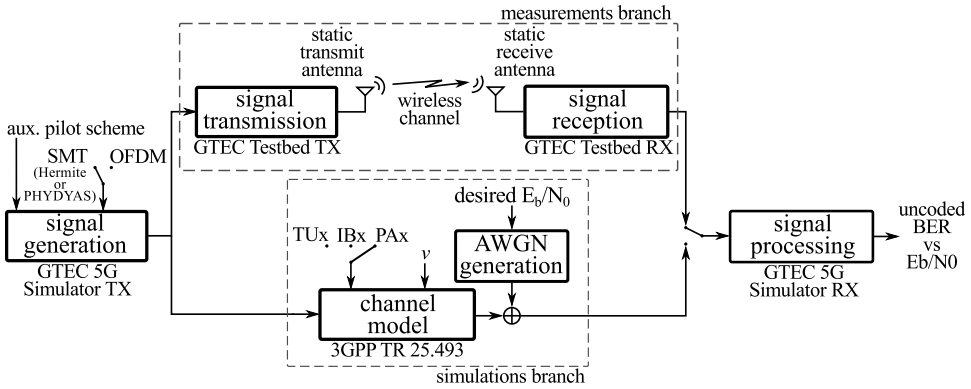

Fig. 1. Block diagram of the setup used for the evaluations. Notice that analytic performance results are also obtained considering AWGN and Rayleigh channel.

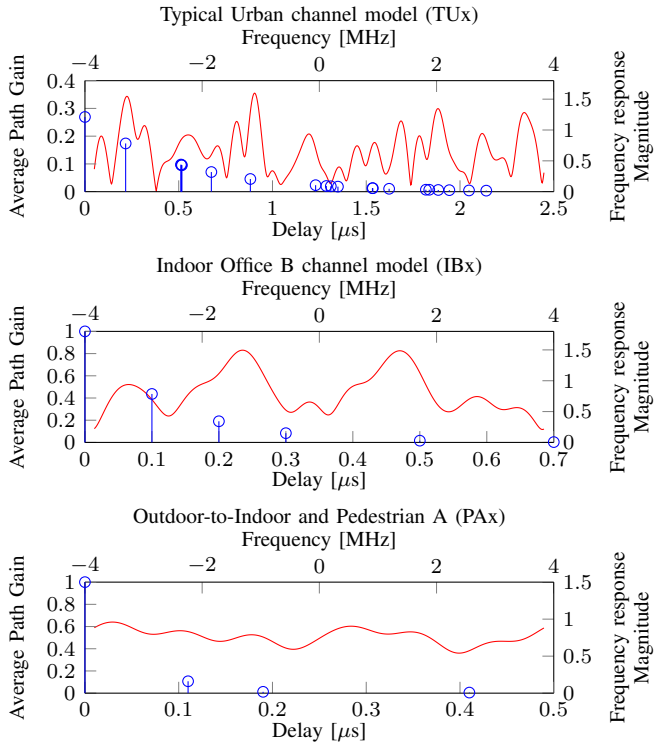

Fig. 2. Power Delay Profile (○) and frequency response (of a realization) (——) of the considered channel models (Typical Urban channel model, Indoor Office B and Outdoor-to-Indoor and Pedestrian A).

C. Testbed Description

The experimental evaluations described in this work are carried out with the testbed developed at our research group and used in previous works [15], [16]. More specifically, we employ two nodes: a transmit-only node and a receive-only node. Each node consists of a USRP B210 board [17] built from the AD9361 chip [18] by Analog Devices, which supports a continuous frequency coverage from 70 MHz to 6 GHz; full-duplex Multiple-Input, Multiple-Output (MIMO) operation with up to two antennas, and a maximum bandwidth of 56 MHz; USB 3.0 connectivity; on-chip 12 bit Analog-to-Digital Converters (ADCs) and Digital-to-Analog Converters (DACs) up to 61.44 Msample/s; and configurable transmit and receive gain values. For each node, its corresponding USRP board is connected to a laptop equipped with two solid-state drives: one containing a GNU/Linux operating system and the custom-developed measurement software, whereas the other is dedicated to storing the transmit/acquired signals.

The transmitter is equipped with two Mini-Circuits TVA-11-422 high-power amplifiers [19], one per antenna. The antennas employed at the transmitter and the receiver nodes, namely MOBILE MARK PSKN3-24/55 [20], are omnidirectional.

With respect to the measurement software, we use a custom-developed multi-threaded software implemented in C++ with Boost [21] and based on the Ettus USRP Hardware Driver (UHD) [22]. At the transmitter side, the samples are first pre-processed and saved into a dedicated solid-state drive. Next, such samples are transmitted over the air in a cyclic fashion using a single antenna at a time from the set of two available. Switching the transmit antenna allows for obtaining different channel realizations from distinct spatial positions and polarizations. At the receiver, the samples coming out of the two antennas (out of the four receive antennas available) of the USRP are read from the USB and stored first in memory, and eventually recorded in a solid state drive. Other important logging information is also stored. Notice that the receiver node acquires signals simultaneously from two different antennas although a Single-Input Single-Output (SISO) system is being assessed. Switching between the two sets, each with two antennas, allows for obtaining different channel realizations.

D. Scenario of the Measurements

In this work we restricted the experimental evaluation to quasi-static scenarios. More specifically, we considered the following scenarios:

1) A medium-sized office represented by the laboratory of our research group at the University of A Coruña. The laboratory is located in the second floor of a building with coordinates $43°19'59.3''$ N, $8°24'33.2''$ W and it occupies an area of 82 m^2. This setup is shown in Fig. 4 and Fig. 6 with transmitter TX1 and receiver RX1 for the case with direct line-of-sight.

2) Transmitter and receiver in static condition with non-line-of-sight in a medium-sized office. This setup is shown in Fig. 4 with transmitter TX2 and receiver RX2. The receiver in this evaluation was in the same location as in the 1).
3) A small office with approximately 19 m^2, represented by a room in the third floor of the aforementioned building, located above the laboratory. This setup is shown in Fig. 5 with transmitter TX3 and receiver RX3.
4) Corridors. Large buildings usually have corridors, which exhibit specific propagation conditions for wireless signals. Therefore, we also consider corridors as typical indoor scenarios. This setup is shown in Fig. 4 and Fig. 7 with transmitter TX4 and receiver RX4 moving at approximately 3 km/h.

IV. Evaluation Procedure

A. Ensuring a Fair Comparison

In order to fairly compare the results for the different considered modulations (OFDM and SMT with Hermite and PHYDYAS pulses), the following aspects were also considered:

- The number of data subcarriers, as well as the subcarrier spacing, are the same in all cases. More specifically, 600 subcarriers are used, while the subcarrier spacing was set to 15 kHz (for the OFDM case, 600 subcarriers are used for a 1024-point FFT). These parameters correspond to the typical configuration for the 10 MHz downlink Long Term Evolution (LTE) profile.
- The pilot density considered for channel estimation is equivalent in all cases. Note that in the case of SMT some additional symbols, namely the APs, are required to minimize the interference caused by the lack of orthogonality of the received pilots [1]. More specifically, a rectangular grid of pilots was used. Such pilot spacing in the time-frequency grid is of 8 subcarriers in the frequency dimension and of 10 symbols in the time dimension for SMT signals (5 symbols in the case of OFDM given that consecutive symbols do not overlap).
- The same algorithms for channel estimation, interpolation and equalization are considered for each of the modulations (see Section III-A).
- A 2-PAM constellation is used for the SMT transmissions, while 4-QAM is considered for OFDM, since the symbols are complex-valued in the latter case.
- The same number of user data bits is considered per transmission. Taking into account that real-valued symbols are used in SMT, whereas complex-valued ones are used for OFDM, more time-positions in the time-frequency grid are required for SMT signals with respect to OFDM for the same number of transmitted bits. However, provided that consecutive SMT symbols partially overlap in the time domain (because a SMT scheme is considered), this does not mean that in order to transmit the same amount of data bits we need twice the time-positions for SMT with respect to OFDM. With the considered model, the user bit rate is approximately the same for both OFDM and SMT, with slight differences caused by the length of the OFDM cyclic prefix and the time dispersion of the prototype filters in SMT.
- Pilot boosting is used. As the pulses are different, the energy allocated for each pilot may be different and the performance of the systems may be different. In Fig. 3 we show the result of a simulation of BER vs pilot boosting factor for OFDM and SMT with an E_b/N_0 of 0 dB. In the figure we can see how SMT starts with a worse performance than OFDM. However, if we increase the pilot boosting we can achieve a better performance and even surpass OFDM. Using this data we decided to use a pilot boosting of 5.5 (7.4 dB) for both OFDM and SMT.
- The signals are scaled to ensure that the transmitted energy per bit is the same for both OFDM and SMT.

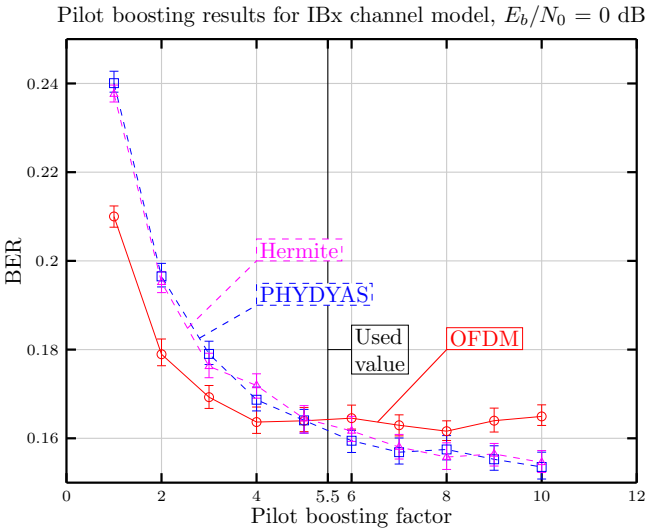

Fig. 3. BER vs pilot boosting factor for E_b/N_0 = 0 and Indoor Office B (IBx) channel model.

We consider the uncoded BER (i.e., the BER after the symbol hard-decision) as the figure of merit for the results evaluation, since it is one of the most used performance metrics in wireless communications.

Finally, Table I details the most relevant parameters considered.

B. Measurement Procedure

Taking advantage of the antenna switching capabilities exhibited by the USRP B210 board and that a SISO system is being considered, eight different channel realizations can be measured without moving the transmit nor the receive node. More channel realizations can be easily obtained by moving the transmitter and the receiver in a small area (typically of $3\,\lambda \times 3\,\lambda$ [23], where λ is the wavelength).

In order to ensure a fair comparison, all waveforms under test are transmitted sequentially under the same conditions (notice that we are assuming quasi-static wireless channels).

TABLE I
MAIN PARAMETERS USED IN THE EXPERIMENTS.

parameter	value
Sampling frequency, F_s	15.36 MHz
FFT size	1024
Number of used subcarriers	600 (excluding DC)
CP length (OFDM)	72 samples
Constellations	2-PAM (SMT) 4-QAM (OFDM)
Pilot spacing	8 subcarriers (frequency dimension) 10 symbols (time dimension, SMT) 5 symbols (time dimension, OFDM)
AP scheme	CAP (8 surrounding symbols)
Pulse overlapping	3 symbols (Hermite) 4 symbols (PHYDYAS)
Velocities, v	0, 3 km/h
Carrier frequency, f_c	2.6 GHz
E_b/N_0	from 0 to 30 dB (simulations)

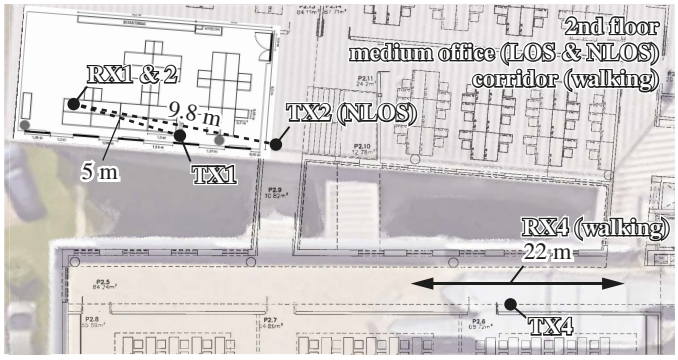

Fig. 4. Map of the second floor of the building where the measurements were performed showing the medium-sized office and corridor scenarios.

V. SIMULATION RESULTS

All the results included in this section are expressed in terms of BER with respect to the E_b/N_0.

- Fig. 8 shows the BER versus E_b/N_0 for the TUx channel model when pedestrian mobility ($v = 3$ km/h) is considered. Additionally, the analytic curves for the AWGN and Rayleigh channel models are included. The BER exhibited by the simulation curves is almost the same (less than 2 dB) for E_b/N_0 values smaller than 20 dB. For large E_b/N_0 values (E_b/N_0 values greater than 20 dB), OFDM performs the best, followed by PHYDYAS, and finally Hermite. This is because the auxiliary pilots are designed for minimizing the interference when an ideal channel is considered. However, depending on the specific channel behavior, the interference caused by the pilot symbols at the receiver can be larger or smaller. The TUx channel model has a high frequency selectivity as shown in Fig. 2, as the PHYDYAS pulse has a more concentrated frequency response than the Hermite one, the interference among the auxiliary pilots its lower and it performs better.
- Fig. 9 shows the same results as Fig. 8 but when the IBx channel model is considered. All the schemes perform similarly although this channels can be equalized easier than those corresponding to the TUx model.
- Fig. 10 shows the same results as Figs. 8 and 9 but when the PAx channel model is considered. As shown in Fig. 2, this channel has a low frequency selectivity, thus the auxiliary pilots of SMT suffer less interference and we can see that SMT performs slighly better.

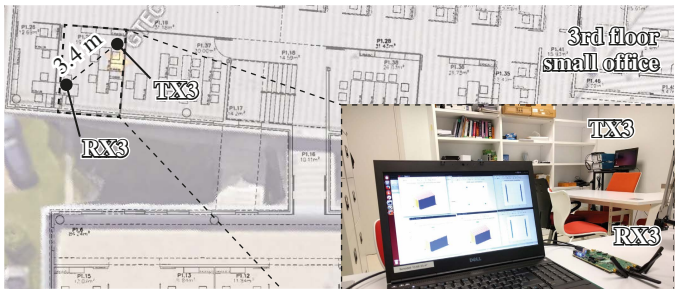

Fig. 5. Map of the third floor of the building where the measurements were performed showing the small office. A picture of the setup is included.

VI. MEASUREMENT RESULTS

Figures 11 to 14 show the results obtained by measurements. All the results are expressed in terms of BER with respect to the E_b/N_0. With the objective of gauging the accuracy of the results, 95 % confidence intervals are also included. Figures 11 and 12 show the results when measuring inside medium and small-sized offices, respectively, under line-of-sight conditions (see Figs. 5 and 6). Figure 13 show the results when placing the receiver inside the medium-sized office and the transmitter at the corridor, thus under non-line-of-sight conditions (see Fig. 4). Finally, Fig. 14 shows the results obtained when the transmitter is located in a corridor and the receiver is moving along the same corridor at a speed of 3 km/h, passing in front of the transmitter (see Fig. 7).

For all the scenarios, the results for the different modulation schemes (OFDM and SMT) are very similar. There is little difference between the results for the considered scenarios for low values of E_b/N_0, since in these cases the noise is the main contributor to the signal distortion. For higher values of E_b/N_0 it can be seen that the performance obtained for the medium-sized office is slightly better than that for the small-sized office (see Figs. 11 and 12). In fact, the results for small-sized office are closer to the analytical results obtained for the Rayleigh channel, which is consistent with the fact that the multipath components are received with more power with respect to the case of the medium-sized office. The results for non-line-of-sight conditions are even closer to the Rayleigh analytical ones (see Fig. 13), as expected. However, it can be seen that there is a lower bound for the BER which is achieved at $E_b/N_0 \approx 12$ dB. According to Fig. 14, the scenario providing the best average performance results is the one in which the receiver is moving. This is because the speed is too low to cause a strong distortion in the signal. On the other hand, as the receiver is

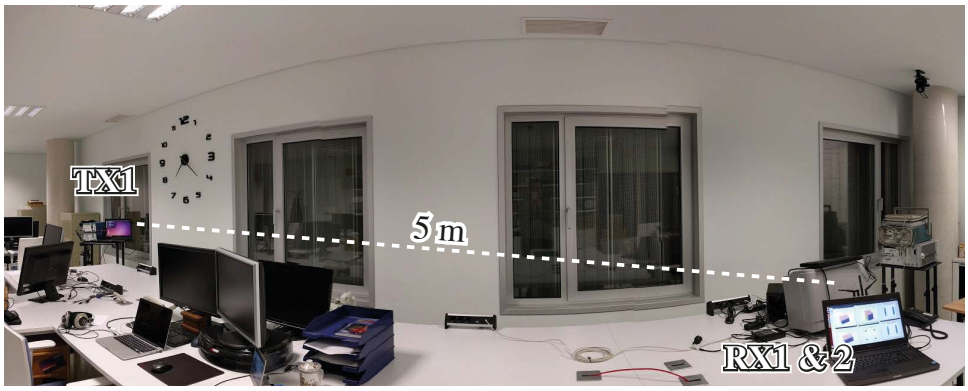

Fig. 6. Picture of the setup for measurements with line-of-sight in a medium-size office.

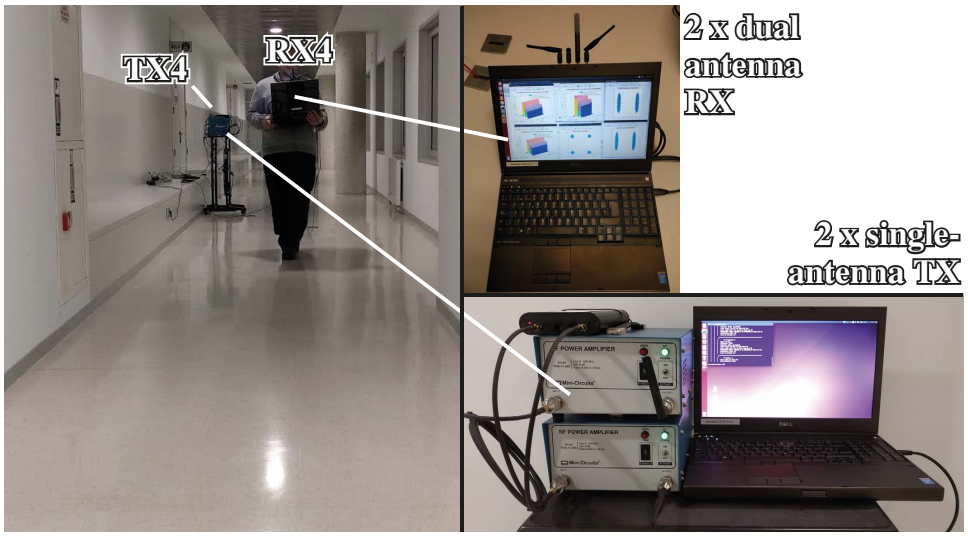

Fig. 7. Picture of the setup for measurements with line-of-sight and receiver moving at 3 km/h in a corridor.

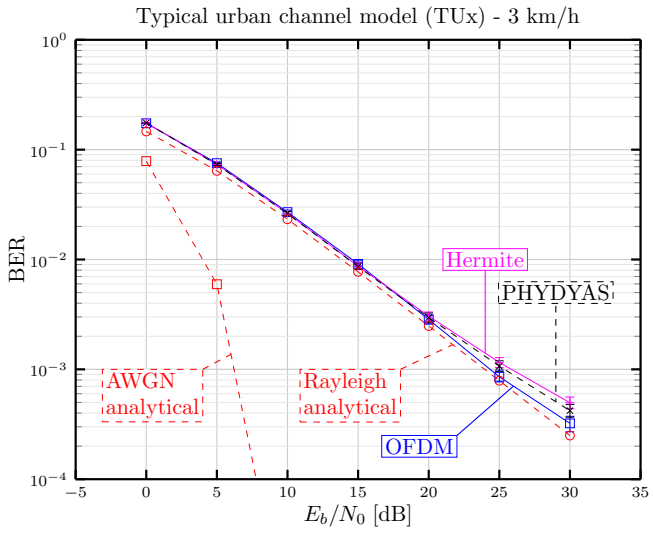

Fig. 8. BER versus E_b/N_0 for the TUx channel model. Pedestrian mobility (3 km/h) is considered.

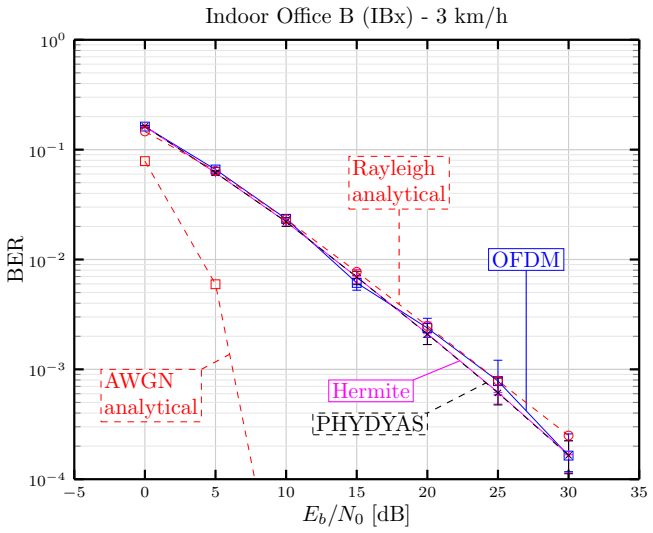

Fig. 9. BER versus E_b/N_0 for the IBx channel model. Pedestrian mobility (3 km/h) is considered. 95 % confidence intervals are shown.

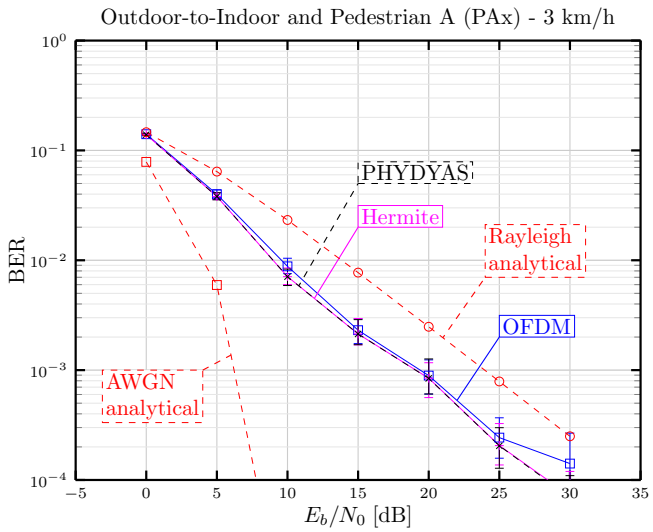

Fig. 10. BER versus E_b/N_0 for the PAx channel model. Pedestrian mobility (3 km/h) is considered. 95 % confidence intervals are shown.

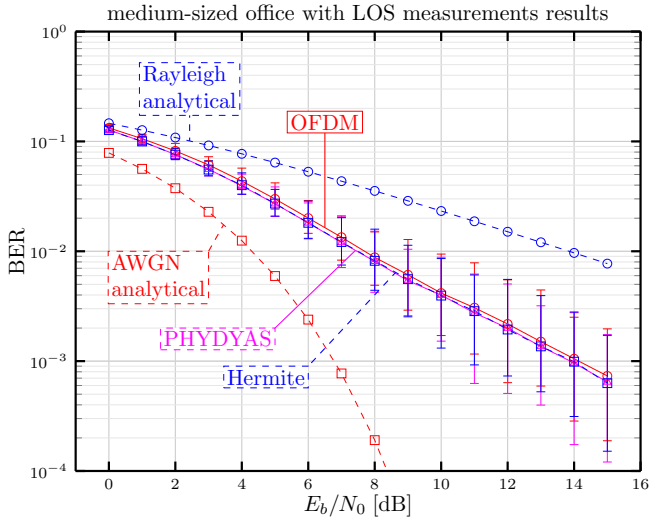

Fig. 11. BER versus E_b/N_0 for the experimental evaluation 1 (Transmitter and receiver in static condition with line-of-sight in a medium size office).

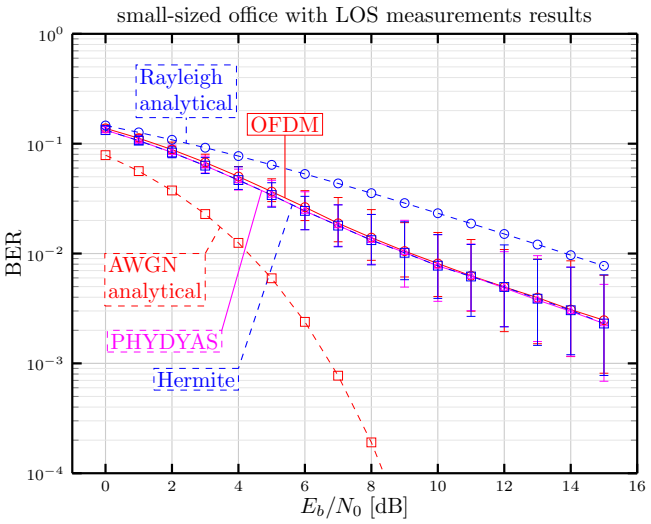

Fig. 12. BER versus E_b/N_0 for the experimental evaluation 3 (Transmitter and receiver in static condition with line-of-sight inside a small size office).

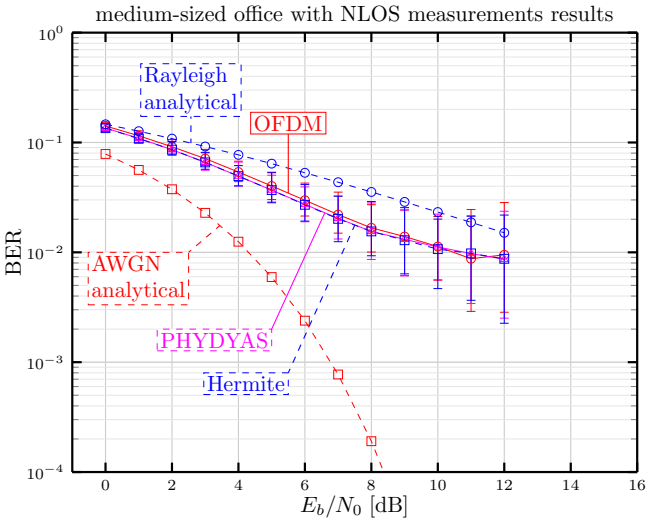

Fig. 13. BER versus E_b/N_0 for the experimental evaluation 2 (Transmitter and receiver in static condition with non-line-of-sight in a medium size office).

moving, when it passes in front of the transmitter the distance between them is very small.

VII. Conclusions

In this work we have compared the performance of two common prototype filters (the one defined by the PHYDYAS project, and the so-called Hermite pulse) for the widely proposed SMT scheme. The performance results were expressed in terms of BER with respect to the E_b/N_0.

We first compared OFDM and SMT by means of computer simulations, assuming perfect time and frequency synchronization between transmitter and receiver. TUx, IBx and PAx channel models were considered with pedestrian mobility ($v = 3$ km/h). Additionally, analytic BER curves were also obtained for the AWGN and Rayleigh channel models.

Finally, several experimental evaluations of OFDM and SMT under different scenarios were performed. We assessed four different quasi-static scenarios considering line-of-sight, non-line-of-sight, and pedestrian mobility ($v = 3$ km/h) situations. Additionally, analytic BER curves were also obtained for the AWGN and Rayleigh channel models.

The main conclusions derived from the results are summarized below.

- A similar performance is obtained for the three modulation schemes considered: OFDM, SMT with the PHYDYAS prototype filter, and SMT with the Hermite prototype filter. This result is confirmed both by simulations and over-the-air transmissions.
- For the considered measurements and simulation scenarios it is possible to use SMT without any performance

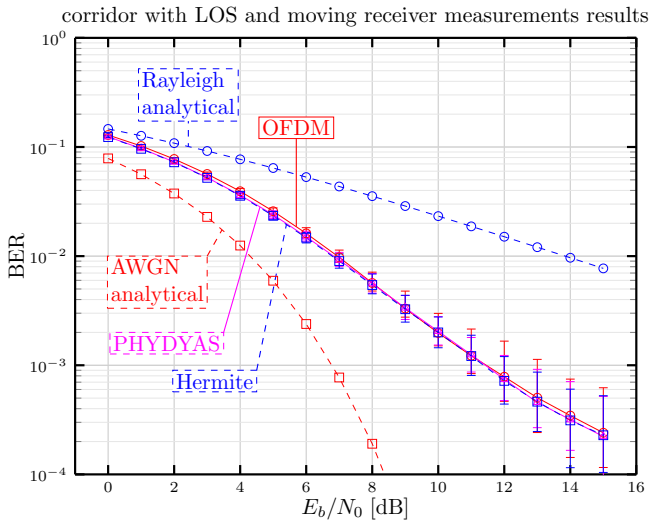

Fig. 14. BER versus E_b/N_0 for the experimental evaluation 4 (Transmitter in static condition and receiver moving at approximately 3 km/h in a corridor).

loss with respect to OFDM. However, it is worth noting that we are not considering any of the potential advantages of SMT, for example, increasing the number of subcarriers for the same spectral mask with respect to OFDM, or the good properties of the Hermite pulse for doubly dispersive channels.

ACKNOWLEDGMENT

This work has been funded by Xunta de Galicia, MINECO of Spain, and FEDER funds of the EU under grants with numbers 2012/287, TEC2013-47141-C4-1-R, FPU12/04139, EST14/00355, BES-2014-069772.

REFERENCES

[1] B. Farhang-Boroujeny, "Ofdm versus filter bank multicarrier," *Signal Processing Magazine, IEEE*, vol. 28, no. 3, pp. 92–112, 2011.

[2] B. L. Floch, M. Alard, and C. Berrou, "Coded orthogonal frequency division multiplex [tv broadcasting]," *Proceedings of the IEEE*, vol. 83, no. 6, pp. 982–996, 1995.

[3] A. Sahin, I. Guvenc, and H. Arslan, "A survey on multicarrier communications: Prototype filters, lattice structures, and implementation aspects," *Communications Surveys & Tutorials, IEEE*, vol. 16, no. 3, pp. 1312–1338, 2012.

[4] J.-P. Javaudin, D. Lacroix, and A. Rouxel, "Pilot-aided channel estimation for ofdm/oqam," in *Vehicular Technology Conference, 2003. VTC 2003-Spring. The 57th IEEE Semiannual*, vol. 3. IEEE, 2003, pp. 1581–1585.

[5] T. H. Stitz, T. Ihalainen, A. Viholainen, and M. Renfors, "Pilot-based synchronization and equalization in filter bank multicarrier communications," *EURASIP Journal on Advances in Signal Processing*, vol. 2010, p. 9, 2010.

[6] W. Cui, D. Qu, T. Jiang, and B. Farhang-Boroujeny, "Coded auxiliary pilots for channel estimation in FBMC-OQAM systems," *IEEE Transactions on Vehicular Technology*, vol. PP, no. 99, pp. 1–1, 2015, doi:10.1109/TVT.2015.2448659.

[7] M. Fuhrwerk, J. Peissig, and M. Schellmann, "Performance comparison of CP-OFDM and OQAM-OFDM systems based on LTE parameters," in *IEEE 10th International Conference on Wireless and Mobile Computing, Networking and Communications (WiMob)*, Oct. 2014, pp. 604–610, doi:10.1109/WiMOB.2014.6962232.

[8] ——, "Channel adaptive pulse shaping for OQAM-OFDM systems," in *Proceedings of the 22nd European Signal Processing Conference (EUSIPCO)*. IEEE, 2014, pp. 181–185.

[9] M. Payaró, A. Pascual-Iserte, and M. Nájar, "Performance comparison between FBMC and OFDM in MIMO systems under channel uncertainty," in *European Wireless Conference (EW), 2010*. IEEE, 2010, pp. 1023–1030, doi:10.1109/EW.2010.5483521.

[10] I. Estella, A. Pascual-Iserte, and M. Payaró, "OFDM and FBMC performance comparison for multistream MIMO systems," in *Future Network and Mobile Summit, 2010*, Jun. 2010, pp. 1–8.

[11] M. Bellanger, D. Le Ruyet, D. Roviras, M. Terré, J. Nossek, L. Baltar, Q. Bai, D. Waldhauser, M. Renfors, T. Ihalainen *et al.*, "Fbmc physical layer: a primer," PHYDYAS FP7 Project Document, Tech. Rep., 2010.

[12] R. Haas and J.-C. Belfiore, "A time-frequency well-localized pulse for multiple carrier transmission," *Wireless Personal Communications*, vol. 5, no. 1, pp. 1–18, 1997.

[13] 3GPP, "3GPP TR 25.943: 3GPP;Technical specification group radio access network; Univerlsal Mobile Telecommunications System (UMTS); Deployment aspects," ETSI, Tech. Rep., December 2004.

[14] ITU-R, "Guidelines for evaluation of radio transmission technologies for IMT-2000. ITU-R Recommendation M.1225," 1997.

[15] J. Rodríguez-Piñeiro, P. Suárez-Casal, J. A. García-Naya, L. Castedo, C. Briso-Rodríguez, and J. I. Alonso-Montes, "Experimental validation of ICI-aware OFDM receivers under time-varying conditions," in *IEEE 8th Sensor Array and Multichannel Signal Processing Workshop (SAM 2014)*, A Coruña, Spain, June 2014.

[16] P. Suárez-Casal, J. Rodríguez-Piñeiro, J. A. García-Naya, and L. Castedo, "Experimental assessment of WiMAX transmissions under highly time-varying channels," in *he Eleventh International Symposium on Wireless Communication Systems (ISWCS)*, Barcelona, Spain, Aug. 2014.

[17] "Ettus USRP B210." [Online]. Available: https://www.ettus.com/product/details/UB210-KIT

[18] "Analog devices AD9361 RFIC." [Online]. Available: http://www.analog.com/en/rfif-components/rfif-transceivers/ad9361/products/product.html

[19] "Mini-circuits high-power amplifier TVA-11-422." [Online]. Available: http://www.minicircuits.com/pdfs/TVA-11-422.pdf

[20] "Mobile mark pskn3-24/55 omnidirectional antenna." [Online]. Available: http://www.mobilemark.com/download/specification-sheets/gps-multi-band/PSKN3-24-55%20%285-6%20GHz%29-pat.pdf.pdf

[21] "Boost C++ libraries." [Online]. Available: http://www.boost.org/

[22] "Ettus USRP hardware driver (UHD)." [Online]. Available: http://files.ettus.com/manual/page_uhd.html

[23] S. Caban, J. A. Garcia-Naya, and M. Rupp, "Measuring the physical layer performance of wireless communication systems: Part 33 in a series of tutorials on instrumentation and measurement," *IEEE Instrumentation and Measurement Magazine*, vol. 14, no. 5, pp. 8–17, Oct. 2011, doi:10.1109/MIM.2011.6041377.